

Discovery and Preclinical Evaluation of [4-[[1-(3-fluorophenyl)methyl]-1*H*-indazol- 5-ylamino]-5-methylpyrrolo[2,1-*f*][1,2,4]triazin- 6-yl]carbamic Acid, (3*S*)-3-Morpholinylmethyl Ester (BMS-599626), a Selective and Orally Efficacious Inhibitor of Human Epidermal Growth Factor Receptor 1 and 2 Kinases

Ashvinikumar V. Gavai,^{*,§} Brian E. Fink,[§]
David J. Fairfax,[‡] Gregory S. Martin,[‡] Lana M. Rossiter,[‡]
Christian L. Holst,[‡] Soong-Hoon Kim,[§] Kenneth J. Leavitt,[§]
Harold Mastalerz,[§] Wen-Ching Han,[§] Derek Norris,[§]
Bindu Goyal,[§] Shankar Swaminathan,[§] Bharat Patel,[§]
Arvind Mathur,[§] Dolatrai M. Vyas,[§] John S. Tokarski,[§]
Chiang Yu,[§] Simone Oppenheimer,[§] Hongjian Zhang,[§]
Punit Marathe,[§] Joseph Fargnoli,[§] Francis Y. Lee,[§]
Tai W. Wong,[§] and Gregory D. Vite[§]

[§]Bristol-Myers Squibb Research and Development,
P.O. Box 4000, Princeton, New Jersey 08543, and
[‡]Albany Molecular Research, 21 Corporate Circle,
P.O. Box 15098, Albany, New York 12212

Received July 8, 2009

Abstract: Structure–activity relationships in a series of 4-[1*H*-indazol-5-ylamino]pyrrolo[2,1-*f*][1,2,4]triazine-6-carbamates identified dual human epidermal growth factor receptor (HER)1/HER2 kinase inhibitors with excellent biochemical potency and kinase selectivity. On the basis of its favorable pharmacokinetic profile and robust *in vivo* activity in HER1 and HER2 driven tumor models, **13** (BMS-599626) was selected as a clinical candidate for treatment of solid tumors.

Receptor tyrosine kinases play a crucial role as signal transducers in dysregulated cell proliferation, differentiation, and evasion from apoptosis. Two members of the epidermal growth factor receptor family, HER1 (EGFR) and HER2 (ErbB2), have been clinically validated as rational targets for cancer therapy.¹ Activation of the HER^a receptors via homo- or heterodimerization is followed by receptor autophosphorylation, recruitment of adaptor proteins, and the activation of downstream signaling, such as those mediated by Ras/Raf/MAPK and the PI3K/Akt pathways.² Overexpression or constitutive activation of HER1 and HER2 has been observed in many tumor types, including colon, breast, ovarian, head and neck, and non-small cell lung cancer, and frequently correlates with poor clinical prognosis.

A number of pharmacologic agents have demonstrated clinical benefit via modulation of HER1 or HER2 receptor.¹ These include HER1-specific antibody cetuximab, HER2-specific antibody trastuzumab, and small molecule HER1 kinase inhibitors gefitinib and erlotinib. Coexpression of HER1 and HER2 kinases has been shown in many tumors,

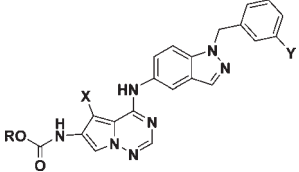
such as breast, ovarian, and bladder tumors, as well as in squamous cell carcinomas of the head and neck.³ Heterodimer signaling is believed to play a significant role in the pathobiology of these tumors. The ability of HER2 to transactivate other receptors of the HER family by heterodimerization suggests that simultaneous inhibition of HER1 and HER2 may provide superior efficacy than single receptor targeting via different and potentially nonoverlapping mechanisms.¹ A high degree of sequence homology (83% identity) between the two kinase domains supports the feasibility of identifying compounds that inhibit both receptors with comparable potency. Lapatinib, an oral dual inhibitor of HER1 and HER2, was recently approved in combination with capecitabine for the treatment of patients with HER2 overexpressing advanced or metastatic breast cancer.⁴

We have previously reported the discovery of pyrrolo[2,1-*f*]-[1,2,4]triazine nucleus as a versatile scaffold for ATP-competitive kinase inhibitors.⁵ Subsequently, we demonstrated that dual inhibitors of HER1 and HER2 kinases can be prepared via introduction of a lipophilic 5-amino-1-benzylindazole substituent at C4 and a carbamate linker at the C6 position of the pyrrolotriazine.⁶ The extended aniline motif conferred improved potency against HER2 while retaining HER1 inhibition. As depicted in Table 1, **1** was the initial lead that exhibited potent inhibition of HER2/HER1 enzymes and submicromolar potency in antiproliferative assays using HER2/HER1-dependent cells. Compound **1** did not show significant activity against HER2/HER1 independent A2780 tumor cells, suggesting thereby that the cellular effects are specific to inhibition of HER kinases. This paper describes further optimization of *in vitro* potency and pharmacokinetic properties leading up to the identification of **13**, a HER1/HER2 kinase inhibitor that has advanced into clinical development.⁷

Previous studies had established that biochemical potency could be improved via optimization of the linker group at C6 position.⁶ In the proposed binding model for the pyrrolotriazine nucleus in the ATP binding site of HER1 kinase, the C6 position points toward a specificity pocket that leads to surface exposed protein.⁶ It was deemed to be an appropriate position to incorporate a polar functionality, such as an aliphatic amine, through the C6 carbamate. This change was predicted to favorably influence physical properties and the pharmacokinetic profile of the kinase inhibitors. To evaluate this hypothesis, a variety of cyclic amines were appended to the pyrrolotriazine using the C6 carbamate linker. As shown in Table 1, the *N*-piperidinylethyl and *N*-piperazinylethyl analogues **2** and **3** displayed the desired increase in potency in HER2 overexpressing BT474 and N87 cell proliferation assays. The corresponding morpholine derivative **4** was less potent in the enzymatic assays. It was expected that sustained inhibition of HER1 and HER2 for a prolonged period of time would be necessary for robust *in vivo* activity in tumor models. To that end, plasma exposures of lead candidates were investigated in mice for 4 h following oral administration. The observed low systemic exposures of **2** and **3** (Table 1) were attributed to a combination of poor absorption and insufficient metabolic stability in isolated liver microsomes.⁸ It has been suggested that the greater polarity

^{*}To whom correspondence should be addressed. Phone: 609-252-5091. Fax: 609-252-3993. E-mail: ashvinikumar.gavai@bms.com.

^a Abbreviations: HER, human epidermal growth factor receptor; MRT, mean residence time; TGI, tumor growth inhibition.

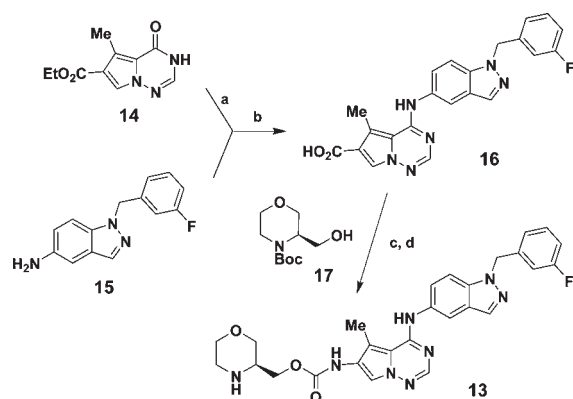
Table 1. Enzymatic and Cellular Activities^a and 4 h Plasma Exposures of Pyrrolotriazine C6 Carbamate Analogues


compd	X	Y	R	kinase inhibition ^b		cellular antiproliferative activity ^b				4h oral exposure ^c (mice)		
				IC ₅₀ , nM HER2	IC ₅₀ , nM HER1	BT474 ^d	IC ₅₀ , nM N87 ^e	Sal2 ^f	A2780 ^g	AUC _(0-4h) nM·h	C _{max} nM	C _{4h} nM
1	Et	H		40	44	860	980	460	>5,000	36,000	9,900	9,900
2	Et	H		38	28	310	390	380	NT ^h	5,500	1,700	1,300
3	Et	H		21	18	71	100	250	NT ^h	620	300	300
4	Et	H		111	77	550	520	500	NT ^h	29,000	11,000	4,900
5	Et	H		23	18	290	540	290	3,780	8,800	2,500	2,500
6	Et	H		19	20	130	170	370	5,220	1,760	480	460
7	Et	H		44	37	130	210	490	NT ^h	530	250	110
8	Et	H		30	23	90	170	130	NT ^h	1,300	450	260
9	Et	H		38	29	310	320	480	3,900	3,600	1,200	1,200
10	Et	H		45	30	470	430	250	4,750	7,200	2,300	2,300
11	Et	H		33	21	420	350	170	4,510	11,000	3,500	2,600
12	Et	F		23	22	190	340	230	8,070	16,250	5,100	5,100
13	Me	F		32	22	310	450	240	>10,000	13,300	4,100	4,100

^a See ref 7b for description of the assay conditions. ^b IC₅₀ values are reported as the mean of three independent determinations. ^c Compounds were formulated as solutions in PEG400/Tween80/water (40:10:50) and administered orally at 50 mg/kg to three Balb/C mice. ^d BT474 is a breast tumor cell line (HER2⁺⁺⁺/HER1⁺). ^e N87 is a gastric tumor cell line (HER2⁺⁺⁺/HER1⁺). ^f Sal2 is a salivary gland tumor cell line with a constitutively active HER2. ^g A2780 is an ovarian tumor cell line (HER2⁻/HER1⁻). ^h NT = not tested.

and basicity of primary and secondary amines relative to the tertiary amine reduce their rate of metabolism by the CYP3A4 isozyme.⁹ Indeed, **5** and **6** showed a significant improvement in metabolic stability⁸ and retained comparable HER1/HER2 inhibitory potency in the in vitro assays. Low C_{max} attained during the exposure study in mice indicated that some of these compounds suffered from poor oral absorption. In the 4-substituted piperidine series, a number of compounds with varying chain length (for example, **7** and **8**) afforded the desired level of potency in the biochemical and cell-based assays. This observation provided further support to the proposed binding hypothesis that C6 substitution extends up to the surface exposed region of the protein.⁶ A one-carbon spacer between piperidine and the carbamate was determined to be optimal to achieve a combination of good in vitro

potency and satisfactory absorption characteristics. Within the isomeric piperidinylmethyl carbamates **8–10**, 2-substituted analogue **10** provided the highest plasma concentration at the end of the 4 h oral exposure study. Previously, we had observed that replacement of the piperidine functionality in **2** with a less basic morpholine (**4**) provided a significant boost to oral absorption, as evidenced by a 6-fold higher C_{max} in the mouse PK study. Indeed, a similar change from **10** to **11** had the intended impact on C_{max}, although magnitude of the increase was less remarkable. Introduction of a fluorine atom at meta-position on the phenyl ring gave **12** with a further boost in the oral exposure in mice via significantly enhanced metabolic stability⁸ and oral absorption. Replacement of C5 ethyl with a methyl group provided **13** with a similar in vitro potency and pharmacokinetic profile. At 10 μM, **13** did not

Scheme 1. Synthesis of **13**^a

^a Reagents and conditions: (a) (1) POCl₃, *i*-Pr₂NEt, toluene, 110 °C; (2) K₂HPO₄, H₂O; (3) **15**, *i*-Pr₂NEt, 70–80 °C; (4) *i*-PrOH, 55–22 °C, 84% overall; (b) (1) aq NaOH (50%), THF–MeOH (8:3), 60 °C; (2) conc HCl, THF, room temperature, 88% overall; (c) **17**, diphenylphosphoryl azide, Et₃N, toluene, 87 °C, 82%; (d) conc HCl, MeOH–H₂O (1:7), 77%.

exhibit significant off-target effects as reflected in its activity on the control A2780 tumor cells. The 4 h plasma levels of **13** in the oral exposure study were more than 100-fold higher than its IC₅₀ for inhibition of HER2/HER1 kinases. Compounds **11**–**13** possess *S*-configuration at the asymmetric center on the morpholine. The corresponding *R*-enantiomers exhibited reduced potency in the cellular assays. Despite its initial promise, further evaluation of **12** was discontinued because of its low bioavailability in higher species (data not shown). On the basis of its promising in vitro potency and pharmacokinetic profile, **13** was selected for further characterization in selectivity, safety, PK, and in vivo efficacy studies.

Compound **13** was synthesized according to the sequence illustrated in Scheme 1.¹⁰ Thus, treatment of intermediate **14**⁶ with phosphorus oxychloride in the presence of diisopropylethylamine afforded the corresponding chloroimide that was condensed with aminoindazole **15**⁶ to give carboxylic acid **16** in 74% overall yield after base-mediated hydrolysis. Curtius rearrangement was accomplished by heating with diphenylphosphoryl azide, and the resulting isocyanate intermediate was trapped with enantiopure alcohol **17**.¹¹ Deprotection of the Boc group under acidic conditions and subsequent crystallization from ethyl acetate afforded **13** in 63% yield from intermediate **16**.

The pharmacokinetic parameters obtained for **13** in four species are summarized in Table 2. The compound has high intrinsic permeability in Caco-2 cells (214 nm/s) and was well absorbed following oral administration from solution formulations at the doses denoted in Table 2. Favorable half-lives (*t*_{1/2}) and mean residence times (MRT) were observed across species with this compound. Systemic clearance¹² was moderate to low compared to the hepatic blood flow for the respective species, and volume of distribution (*V*_{ss}) was larger than total body water, indicating extensive extravascular distribution. The measured oral bioavailability (*F*_{po}) ranged from 31% in cynomolgus monkey to 83% in mice.

In addition to potent inhibition of HER1 and HER2, **13** weakly inhibited the related receptor HER4 with an IC₅₀ of 190 nM and exhibited greater than 100-fold selectivity against a panel of diverse protein kinases.^{7b} In N87, Sal2, and GEO tumor cells with activated HER2 and/or HER1 receptors, **13**

Table 2. Pharmacokinetic Parameters for **13**

parameter	mouse ^a	rat ^a	dog ^b	monkey ^b
po dose (mg kg ⁻¹)	120 ^c	10 ^d	25 ^d	5 ^d
iv dose (mg kg ⁻¹)	25 ^c	2.5 ^d	1.5 ^d	5 ^d
<i>C</i> _{max} (μM), po	18	0.6	1.2	0.5
<i>T</i> _{max} (h), po	1.0	0.7	2.3	1.5
AUC ^e (μM.h), po	147	2.9	14.0	3.6
plasma <i>t</i> _{1/2} (h), po	2.7	2.8	7.2	5.7
MRT (h), iv	3.7	2.8	6.9	6.4
Cl, (mL min ⁻¹ kg ⁻¹), iv	21.3	41.6	24.8	10.5
<i>V</i> _{ss} (L kg ⁻¹), iv	4.7	5.7	10.1	4.0
<i>F</i> _{po} (%)	83	40	49	31

^a Data reported as an average of three animals. ^b Data reported as an average of two animals. ^c Vehicle: PG/ Tween80/ water (40:10:50). ^d Vehicle: PEG400/Tween80/water (50:0.1:50). ^e AUC_(0–24h).

Table 3. In Vivo Antitumor Activity of **13** against L2987, GEO, KPL4, and N87 Tumor Xenografts

tumor model	dose ^a (mg kg ⁻¹)	schedule	TGI ^b (%)	<i>P</i> ^c
L2987	30	q.d. × 14	≤50	0.1480
	60	q.d. × 14	58	0.0001
	180	q.d. × 14	99	0.0001
GEO	60	q.d. × 14	39	0.2043
	120	q.d. × 14	95	0.0001
	180	q.d. × 14	88	0.0001
KPL4	60	q.d. × 21	61	0.0001
	180	q.d. × 21	129	0.0019
N87	60	q.d. × 21	39	0.2043
	120	q.d. × 21	81	0.0003
	180	q.d. × 21	71	0.0005

^a Vehicle: propylene glycol/Tween80/water (40:10:50). ^b Percent tumor growth inhibition (TGI) during treatment. ^c Probability of mean tumor weight at the end of drug treatment.

elicited dose-dependent inhibition of receptor phosphorylation and downstream signaling through Akt and MAPK pathways. The potency of this inhibition was consistent with the potency observed for inhibition of cell proliferation. Furthermore, 1 μM **13** inhibited epidermal growth factor dependent HER1/HER2 heterodimer formation in AU565 breast cancer cells.^{7b}

Results for the in vivo activity of **13** in L2987 human lung, GEO human colon, KPL4 human breast, and N87 human gastric carcinoma xenograft models are summarized in Table 3. In the L2987 tumors that are dependent on HER1 signaling, once daily oral administration of **13** resulted in a dose-dependent inhibition of tumor growth (Figure 1).¹³ At 60 mg/kg, the compound achieved a significant delay in tumor growth during the course of treatment. Nearly complete tumor stasis was observed throughout the dosing regimen at the 180 mg/kg dose level, but tumor growth resumed following the cessation of treatment. **13** exhibited similar antitumor activity in HER1-overexpressing GEO tumors and HER2-amplified xenograft models, including KPL4 breast and N87 gastric tumors. No overt toxicity as measured by significant weight loss or morbidity was observed at any of the dose levels tested in these experiments.

In conclusion, optimization of the in vitro potency and pharmacokinetic profile of a series of substituted 4-[1*H*-indazol-5-ylamino]-pyrrolo[2,1-*f*][1,2,4]triazine-6-carbamates led to the identification of **13**, a selective dual inhibitor of HER1 and HER2 kinases, which was orally efficacious in human HER1 (GEO, L2987) or HER2 (KPL4, N87) dependent tumor xenograft models at multiple dose levels. On the

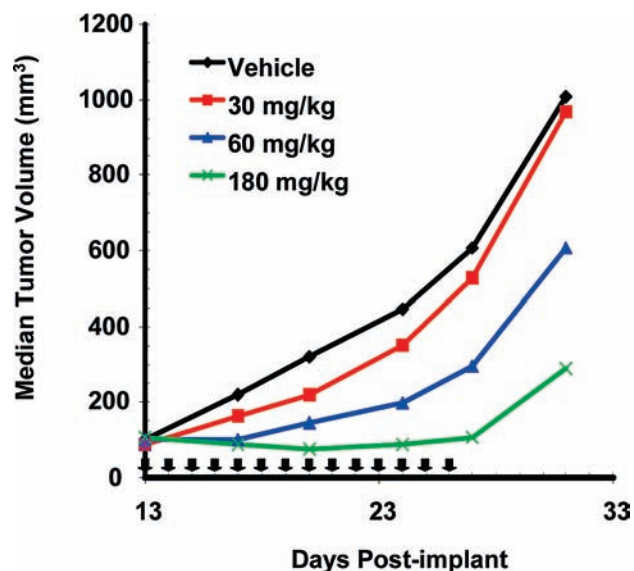


Figure 1. In vivo efficacy of **13** (q.d. \times 14, po) versus L2987 human tumor xenografts in athymic mice.

basis of its favorable in vitro pharmacology, broad spectrum in vivo efficacy in multiple tumor models, and a satisfactory pharmacokinetic profile, **13** was advanced into clinical trials.

Acknowledgment. We thank Bristol-Myers Squibb Discovery Analytical Sciences Department for compound characterization efforts.

Supporting Information Available: Full experimental procedures and characterization data for **13**; characterization data for **1–12**. This material is available free of charge via the Internet at <http://pubs.acs.org>.

References

- (1) (a) Hynes, N. E.; Lane, H. A. ERBB receptors and cancer: the complexity of targeted inhibitors. *Nat. Rev. Cancer* **2005**, *5*, 341–354. (b) Baselga, J.; Arteaga, C. L. Critical update and emerging trends in epidermal growth factor receptor targeting in cancer. *J. Clin. Oncol.* **2005**, *23*, 2445–2459.
- (2) Yarden, Y.; Sliwkowski, M. X. Untangling the ErbB signaling network. *Nat. Rev. Mol. Cell Biol.* **2001**, *2*, 127–137.
- (3) (a) Skirnisdottir, I.; Sorbe, B.; Seidal, T. The growth factor receptors HER-2/neu and EGFR, their relationship, and their effects on the prognosis in early stage (FIGO I-II) epithelial ovarian carcinoma. *Int. J. Gynecol. Cancer* **2001**, *11*, 119–129. (b) Xia, W.; Lau, Y. K.; Zhang, H. Z.; Xiao, F. Y.; Johnston, D. A.; Liu, A. R.; Li, L.; Katz, R. L.; Hung, M. C. Combination of EGFR, HER-2/neu, and HER-3 is a stronger predictor for the outcome of oral squamous cell carcinoma than any individual family members. *Clin. Cancer Res.* **1999**, *5*, 4164–4174.
- (4) Moy, B.; Kirkpatrick, P.; Kar, S.; Goss, P. Lapatinib. *Nat. Rev. Drug Discovery* **2007**, *6*, 431–432.
- (5) Hunt, J. T.; Mitt, T.; Borzilleri, R.; Gullo-Brown, J.; Fagnoli, J.; Fink, B.; Han, W.-C.; Mortillo, S.; Vite, G.; Wautlet, B.; Wong, T.; Yu, C.; Zheng, X.; Bhide, R. Discovery of pyrrolo[2,1-f][1,2,4]-triazine nucleus as a new kinase inhibitor template. *J. Med. Chem.* **2004**, *47*, 4054–4059.
- (6) Fink, B. E.; Vite, G. D.; Mastalerz, H.; Kadow, J. F.; Kim, S.-H.; Leavitt, K. J.; Du, K.; Crews, D.; Mitt, T.; Wong, T. W.; Hunt, J. T.; Vyas, D. M.; Tokarski, J. S. New dual inhibitors of EGFR and HER2 protein tyrosine kinase. *Bioorg. Med. Chem. Lett.* **2005**, *15*, 4774–4779.
- (7) (a) Presented in part at the “First Time Disclosure of Clinical Candidates Symposium”, 229th National Meeting of the American Chemical Society, San Diego, CA, March **2005**; MEDI 21. (b) Wong, T. W.; Lee, F. Y.; Yu, C.; Luo, F. R.; Oppenheimer, S.; Zhang, H.; Smykla, R. A.; Mastalerz, H.; Fink, B. E.; Hunt, J. T.; Gavai, A. V.; Vite, G. D. Preclinical antitumor activity of BMS-599626, a pan-HER kinase inhibitor that inhibits HER1/HER2 homodimer and heterodimer signaling. *Clin. Cancer Res.* **2006**, *12*, 6186–6193.
- (8) The rates of metabolism of **2**, **3**, **5**, **6**, **11**, **12**, and **13** in mouse liver microsomes were 0.27, 0.10, 0.04, 0.02, 0.14, 0.01, and 0.02 nmol min⁻¹ mg protein⁻¹, respectively, after a 10 min incubation at 10 μ M.
- (9) Smith, D. A.; Jones, C. J.; Walker, D. K. Design of drugs involving the concepts and theories of drug metabolism and pharmacokinetics. *Med. Res. Rev.* **1996**, *16*, 243–266.
- (10) Swaminathan, S.; Gavai, A. V.; Fan, J.; Patel, B. P.; Norris, D. J.; Corbett, R. M.; Zheng, B. WO Patent Application 058245 A2, **2005**.
- (11) Brown, G. R.; Foubister, A. J.; Wright, B. Chiral synthesis of 3-substituted morpholines via serine enantiomers and reductions of 5-oxomorpholine-3-carboxylates. *J. Chem. Soc., Perkin Trans. 1* **1985**, 2577–2580.
- (12) Observed systemic clearance of **13** correlated with in vitro clearance in hepatocytes. The predicted hepatocyte clearance values in mouse, rat, monkey, dog, and human were 62.6, 35.6, 18.3, 17.9, and 6.3 mL/min/kg, respectively.
- (13) Tumors were implanted subcutaneously in athymic mice and staged to approximately 100–150 mm³ prior to the initiation of drug treatment. The compound was evaluated on a once daily (q.d.) oral dosing regimen for 14 consecutive days. An active result in these studies is defined as >50% TGI over at least one tumor volume doubling time. For additional experimental details, see the following: Borzilleri, R. M.; Zheng, X.; Qian, L.; Ellis, C.; Cai, Z.-w.; Wautlet, B. S.; Mortillo, S.; Jeyaseelan, R.; Sr.; Kukral, D. W.; Fura, A.; Kamath, A.; Vyas, V.; Tokarski, J. S.; Barrish, J. C.; Hunt, J. T.; Lombardo, L. J.; Fagnoli, J.; Bhide, R. S. Design, synthesis, and evaluation of orally active 4-(2,4-difluoro-5-(methoxycarbonyl)phenylamino)pyrrolo[2,1-f][1,2,4]triazines as dual vascular endothelial growth factor receptor-2 and fibroblast growth factor receptor-1 inhibitors. *J. Med. Chem.* **2005**, *48*, 3991–4008.